

# Is SAM 2 Better than SAM in Medical Image Segmentation?

Sourya Sengupta<sup>1\*</sup>, Satrajit Chakrabarty<sup>1\*</sup>, and Ravi Soni<sup>1</sup>

<sup>1</sup>GE HealthCare, San Ramon, CA, United States

\* denotes equal contributions

**Abstract.** The Segment Anything Model (SAM) has demonstrated impressive performance in zero-shot promptable segmentation on natural images. The recently released Segment Anything Model 2 (SAM 2) claims to outperform SAM on images and extends the model’s capabilities to video segmentation. Evaluating the performance of this new model in medical image segmentation, specifically in a zero-shot promptable manner, is crucial. In this work, we conducted extensive studies using multiple datasets from various imaging modalities to compare the performance of SAM and SAM 2. We employed two point-prompt strategies: (i) multiple positive prompts where one prompt is placed near the centroid of the target structure, while the remaining prompts are randomly placed within the structure, and (ii) combined positive and negative prompts where one positive prompt is placed near the centroid of the target structure, and two negative prompts are positioned outside the structure, maximizing the distance from the positive prompt and from each other. The evaluation encompassed 24 unique organ-modality combinations, including abdominal structures, cardiac structures, fetal head images, skin lesions and polyp images across 11 publicly available MRI, CT, ultrasound, dermoscopy, and endoscopy datasets. Preliminary results based on 2D images indicate that while SAM 2 may perform slightly better in a few cases, it does not generally surpass SAM for medical image segmentation. Notably, SAM 2 performs worse than SAM in lower contrast imaging modalities, such as CT and ultrasound. However, for MRI images, SAM 2 performs on par with or better than SAM. Like SAM, SAM 2 also suffers from over-segmentation issues, particularly when the boundaries of the target organ are fuzzy.

**Keywords:** Foundation models · Interactive segmentation · SAM 2 · SAM · Medical Imaging · Multi-modality.

## 1 Introduction

The recently released Segment Anything Model (SAM) by Meta has demonstrated impressive interactive and promptable image segmentation performance across various computer vision tasks [1]. The original SAM model was trained on a large corpus of data comprising 11 million image-mask pairs, which has enabled it to exhibit efficient, generalizable zero-shot performance on unseen data. While

SAM has shown remarkable results on natural images, it is crucial to evaluate its performance on medical images, where contrast, texture, and shapes differ significantly from those in natural images. Recent efforts have been made to assess SAM’s capabilities on medical images, fine-tune the model with medical data, perform modality-specific fine-tuning, and incorporate novel and diverse prompting strategies to enhance its performance [2,3,4,5,6,7,8]. Meta has recently introduced the Segment Anything Model 2 (SAM 2) [9], an updated version of SAM that extends its capabilities to include both promptable 2D image segmentation and video segmentation.

This work focuses on comparing SAM and SAM 2 specifically in the context of 2D image segmentation. Although the main innovation of SAM 2 lies in its ability to perform video segmentation, it is important to evaluate whether it serves as a better alternative to the original SAM for 2D medical image segmentation. Various click-prompt strategies, including both positive and negative prompts, are explored in this study. A total of 24 different organs/pathologies are segmented from 11 publicly available datasets across five different medical imaging modalities.

## 2 Methods

### 2.1 SAM Model

The Segment Anything Model (SAM) architecture consists of three main components: the image encoder, the prompt encoder, and the mask decoder. The image encoder is built on a Vision Transformer (ViT) architecture [10], which extracts high-level features from the input images. The ViT processes these images by dividing them into smaller patches and applying a series of transformer layers to capture spatial and semantic information. The prompt encoder is designed to handle various types of user inputs, such as points, boxes, or text, to guide the segmentation process. It processes the prompts and encodes them into a feature space that aligns with the image features extracted by the image encoder. The mask decoder is responsible for generating the final segmentation prediction. It combines the features from both the image encoder and the prompt encoder to produce the segmentation output. The mask decoder employs a Two-Way Transformer to integrate these features and includes an IoU (Intersection over Union) head, which predicts the quality of the segmentation mask.

### 2.2 SAM 2 Model

The SAM 2 architecture is designed to extend the capabilities of the original SAM by supporting video segmentation and object tracking in temporal sequences. Unlike SAM, which focuses on individual frame segmentation, SAM 2 incorporates several new components specifically to handle video data. These components include memory attention, a memory encoder, and a memory bank. The memory attention block employs multiple attention layers to integrate features and predictions from previous frames, while the memory encoder creates and stores

these memories in a memory bank for future reference. By conditioning frame embeddings on both past and future frames, SAM 2 is able to maintain temporal coherence across video sequences. Additionally, SAM 2’s prompt encoder and mask decoder can process spatial prompts and iteratively refine segmentation masks. However, for single-frame image segmentation, SAM and SAM 2 perform similarly. SAM 2 uses the same promptable mask decoder as SAM to process frame and prompt embeddings, but without the added temporal conditioning features necessary for video segmentation.

### 2.3 Different Prompting Strategies

For all analyses in the current work, point prompts are utilized and applied in two distinct ways:

- Multiple positive prompts: One prompt is placed near the centroid of the target structure, while the remaining prompts are randomly placed within the structure.
- Combined positive and negative prompts: One positive prompt is placed near the centroid of the target structure, and two negative prompts are positioned outside the structure, maximizing the distance from the positive prompt and from each other.

## 3 Results

### 3.1 Datasets

The models are evaluated on 11 publicly available datasets.

Table 1: Descriptions of various medical imaging datasets used for evaluation.

Dataset Name	Modality	Description
AMOS-CT [11]	CT	Abdominal organs
CHAOS-CT [12]	CT	Abdominal organs
TotalSegmentatorV2-CT [13]	CT	Whole body organs
AMOS-MRI [11]	MRI	Abdominal organs
CHAOS-MRI [12]	MRI	Abdominal organs
TotalSegmentatorV2-MRI [14]	MRI	Whole body organs
CAMUS [15]	Ultrasound	Left ventricle endocardium, left atrium
FH-PS-AOP [16]	Ultrasound	Fetal head
HC [17]	Ultrasound	Fetal head circumference
ISIC [18,19,20]	Dermoscopy	Skin cancer
BKAI-IGH NeoPolyp [21]	Endoscopy	Polyp

These include CT (AMOS [11], CHAOS [12], TotalSegmentatorV2 [13]), MRI (AMOS [11], CHAOS [12], TotalSegmentatorV2 [14]), Ultrasound (CAMUS [15], HC [17], FH-PS-AOP [16], Breast Ultrasound Dataset [22]), Dermoscopy (ISIC [18,19,20]), and Endoscopy (BKAI-IGH NeoPolyp [21,23]) datasets.

For both CT and MRI, we focused on the following abdominal organs: left kidney, right kidney, liver, bladder, gall bladder, spleen, aorta, pancreas, prostate. For ultrasound, dermoscopy, and endoscopy, all structures available in the datasets were included. For CT, MRI, and Ultrasound, data were preprocessed by min-max normalization using the 0.5 and 99.5 percentiles of the image intensities and then scaled to  $[0, 255]$  intensity range. For endoscopy and dermoscopy, intensity values were unchanged. Results are presented for various organs across these datasets (Figures 1–4).

### 3.2 Quantitative Comparison for only positive prompts

Figure 1 shows a quantitative comparison between SAM and SAM 2 on different datasets of MRI, CT, Ultrasound, Dermoscopy and Endoscopy for increasing number of positive prompts.

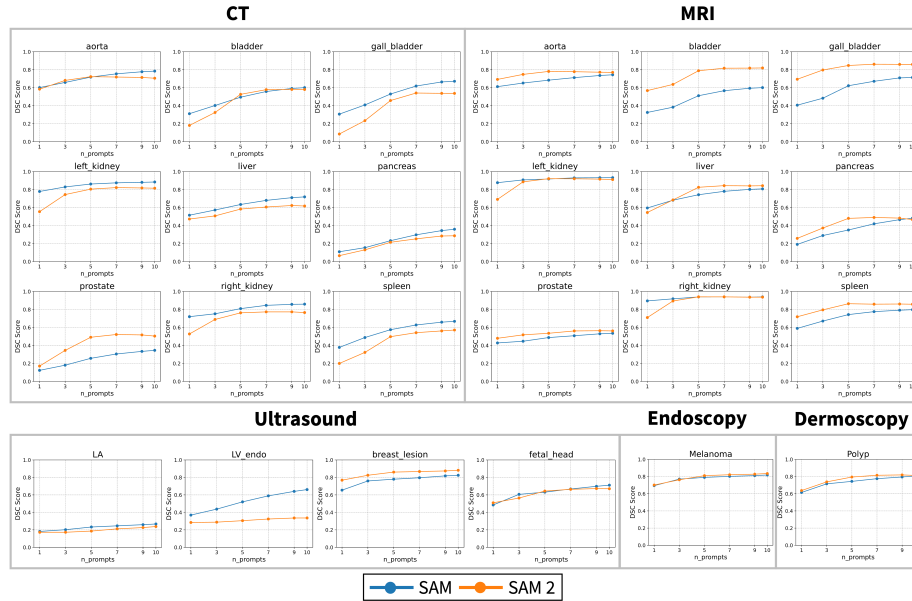


Fig. 1: Performance trends of SAM and SAM 2 in terms of Dice Similarity Coefficient (DSC) with 1, 3, 5, 7, 9, and 10 positive prompts.

For each modality and organ, dice scores are averaged across different datasets and shown in each line plot. For both SAM and SAM 2, there is a general increasing trend in performance with increasing click prompts. In comparison of both models, SAM 2 performs consistently worse than SAM for CT and Ultrasound. However, SAM 2 can surpass the performance of SAM in few cases, especially in higher contrast modality like MRI. For Dermoscopy and Endoscopy SAM 2 performs

very similarly with SAM. Figure 2 shows qualitative performance across multiple modalities for a single positive prompt.

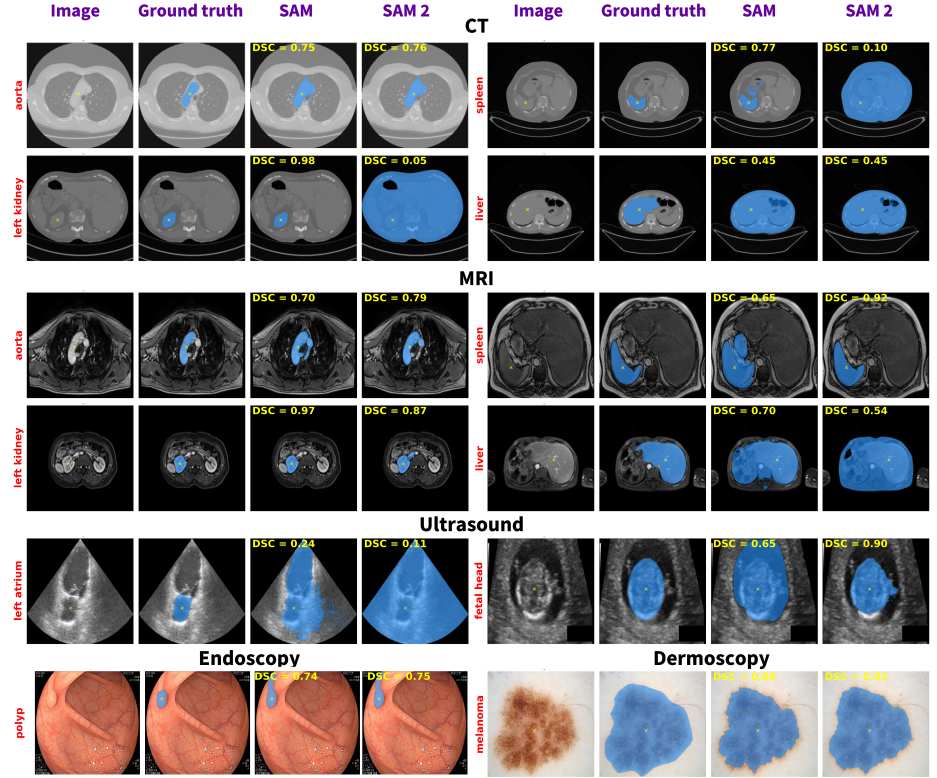


Fig. 2: Qualitative comparison of SAM vs. SAM 2 performance along with the Dice Similarity Coefficient (DSC) values for different structures across all modalities. All results shown are for a single positive prompt (denoted by  $\times$  in the images).

### 3.3 Quantitative Comparison for positive and negative prompts

In this study positive click prompt is combined with two negative prompts. The positive prompt is given near the centroid of the object and two negative prompts are given in two different sides of the positive prompt. Figure 3 shows the trend of dice score for both SAM and SAM 2. The general trend shows that negative prompts boost the performance for both SAM and SAM 2 significantly. For SAM 2, the performance gain with negative prompt can be more significant than SAM. This finding, combined with the performance trend shown in Figure 1, signifies that SAM 2 has a potential drawback of missing the boundary (especially when the contrast is less) but with the help of negative prompts it can generalize

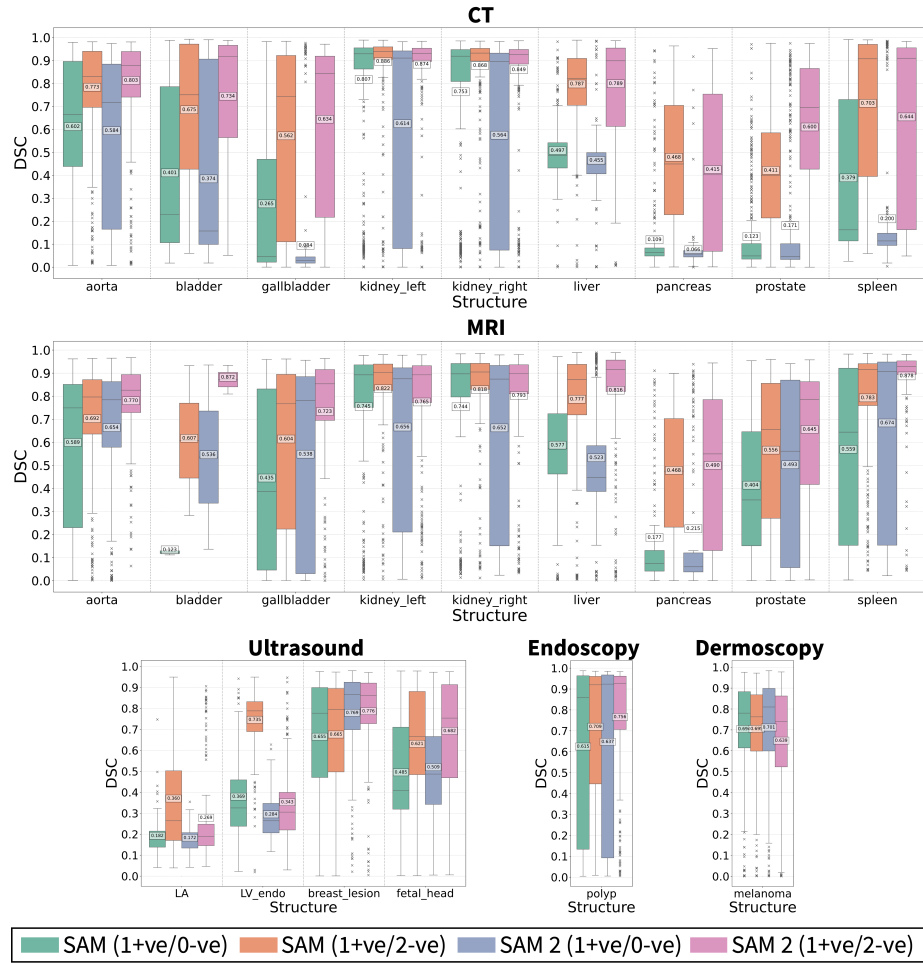


Fig. 3: Quantitative comparison of SAM vs. SAM 2 performance in terms of Dice Similarity Coefficient (DSC) per structure across datasets. For both models, performance is shown for (1 positive, 0 negative) prompt and (1 positive, 2 negative) prompts.

significantly better. Figure 4 shows qualitative performance for four different structures from CT, MRI, Ultrasound and Endoscopy modalities for a single positive prompt and single positive with two negative prompts.

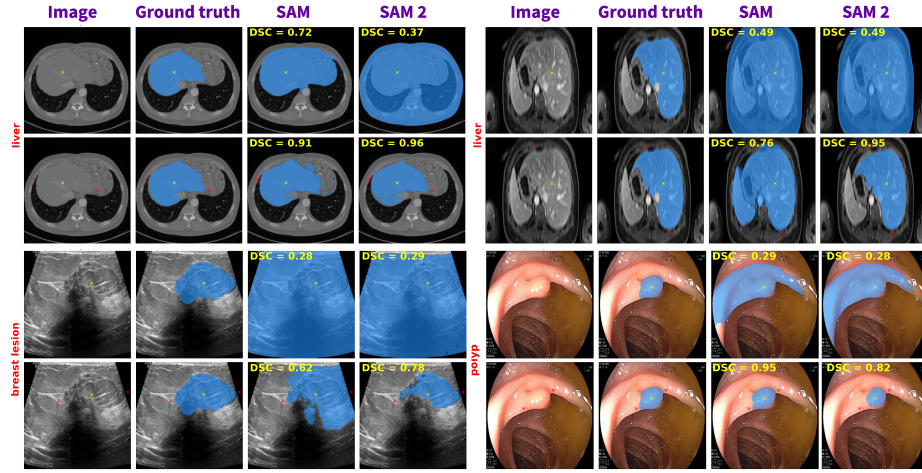


Fig. 4: Qualitative comparison of SAM vs. SAM 2 performance along with the Dice Similarity Coefficient (DSC) values for four structures, one each from CT, MRI, Ultrasound and Endoscopy modalities. For each subplot, the top and bottom rows show results for (1 positive, 0 negative) prompt and (1 positive, 2 negative) prompts respectively. Positive and negative prompts are respectively denoted by  $\times$  and  $\times$  in the images.

## 4 Conclusion

In this work a systematic evaluation study is performed to compare performance of SAM and SAM 2. In future studies a more thorough analysis will be performed with 3D medical images and timelapse videos of bio-imaging. The major observations are

- SAM 2 performs worse in CT, Ultrasound but performs slightly better for MRI. It performs similar to SAM for Dermoscopy, Endoscopy. This shows SAM 2 is relatively a poorer choice for low contrast medical imaging modalities.
- With the help of negative prompts, in most cases SAM 2 performs either very similar or better than SAM.

## References

1. A. Kirillov, E. Mintun, N. Ravi, H. Mao, C. Rolland, L. Gustafson, T. Xiao, S. Whitehead, A. C. Berg, W.-Y. Lo *et al.*, “Segment anything,” in *Proceedings of the IEEE/CVF International Conference on Computer Vision*, 2023, pp. 4015–4026. [1](#)
2. J. Ma *et al.*, “Segment anything in medical images,” *Nature Communications*, vol. 15, no. 1, p. 654, 2024. [2](#)
3. H. Ravishankar *et al.*, “Sonosam-segment anything on ultrasound images,” in *International Workshop on Advances in Simplifying Medical Ultrasound*. Springer Nature Switzerland, 2023. [2](#)

4. Y. Huang, X. Yang, L. Liu, H. Zhou, A. Chang, X. Zhou, R. Chen, J. Yu, J. Chen, C. Chen *et al.*, “Segment anything model for medical images?” *Medical Image Analysis*, vol. 92, p. 103061, 2024. 2
5. J. Wu, W. Ji, Y. Liu, H. Fu, M. Xu, Y. Xu, and Y. Jin, “Medical sam adapter: Adapting segment anything model for medical image segmentation,” *arXiv preprint arXiv:2304.12620*, 2023. 2
6. C. Li, P. Khanduri, Y. Qiang, R. I. Sultan, I. Chetty, and D. Zhu, “Auto-prompting sam for mobile friendly 3d medical image segmentation,” *arXiv preprint arXiv:2308.14936*, 2023. 2
7. S. Gong, Y. Zhong, W. Ma, J. Li, Z. Wang, J. Zhang, P.-A. Heng, and Q. Dou, “3dsam-adapter: Holistic adaptation of sam from 2d to 3d for promptable medical image segmentation,” *arXiv preprint arXiv:2306.13465*, 2023. 2
8. C. Chen, J. Miao, D. Wu, Z. Yan, S. Kim, J. Hu, A. Zhong, Z. Liu, L. Sun, X. Li *et al.*, “Ma-sam: Modality-agnostic sam adaptation for 3d medical image segmentation,” *arXiv preprint arXiv:2309.08842*, 2023. 2
9. N. Ravi, V. Gabeur, Y.-T. Hu, R. Hu, C. Ryali, T. Ma, H. Khedr, R. Rädle, C. Rolland, L. Gustafson *et al.*, “Sam 2: Segment anything in images and videos,” *arXiv preprint arXiv:2408.00714*, 2024. 2
10. A. Dosovitskiy, L. Beyer, A. Kolesnikov, D. Weissenborn, X. Zhai, T. Unterthiner, M. Dehghani, M. Minderer, G. Heigold, S. Gelly *et al.*, “An image is worth 16x16 words: Transformers for image recognition at scale,” *arXiv preprint arXiv:2010.11929*, 2020. 2
11. Y. Ji, H. Bai, C. Ge, J. Yang, Y. Zhu, R. Zhang, Z. Li, L. Zhanng, W. Ma, X. Wan *et al.*, “Amos: A large-scale abdominal multi-organ benchmark for versatile medical image segmentation,” *Advances in neural information processing systems*, vol. 35, pp. 36 722–36 732, 2022. 3
12. A. E. Kavur, N. S. Gezer, M. Barış, S. Aslan, P.-H. Conze, V. Groza, D. D. Pham, S. Chatterjee, P. Ernst, S. Özkan *et al.*, “Chaos challenge-combined (ct-mr) healthy abdominal organ segmentation,” *Medical Image Analysis*, vol. 69, p. 101950, 2021. 3
13. J. Wasserthal, H.-C. Breit, M. T. Meyer, M. Pradella, D. Hinck, A. W. Sauter, T. Heye, D. T. Boll, J. Cyriac, S. Yang *et al.*, “Totalsegmentator: robust segmentation of 104 anatomic structures in ct images,” *Radiology: Artificial Intelligence*, vol. 5, no. 5, 2023. 3
14. T. A. D’Antonoli, L. K. Berger, A. K. Indrakanti, N. Vishwanathan, J. Weiß, M. Jung, Z. Berkarda, A. Rau, M. Reisert, T. Küstner *et al.*, “Totalsegmentator mri: Sequence-independent segmentation of 59 anatomical structures in mr images,” *arXiv preprint arXiv:2405.19492*, 2024. 3
15. S. Leclerc *et al.*, “Deep learning for segmentation using an open large-scale dataset in 2d echocardiography,” *IEEE transactions on medical imaging*, vol. 38, no. 9, pp. 2198–2210, 2019. 3
16. Y. Lu *et al.*, “The jnu-ifm dataset for segmenting pubic symphysis-fetal head,” *Data in brief*, vol. 41, p. 107904, 2022. 3
17. T. L. van den Heuvel *et al.*, “Automated measurement of fetal head circumference using 2d ultrasound images,” *PloS one*, vol. 13, no. 8, p. e0200412, 2018. 3
18. N. C. Codella, D. Gutman, M. E. Celebi, B. Helba, M. A. Marchetti, S. W. Dusza, A. Kalloo, K. Liopyris, N. Mishra, H. Kittler *et al.*, “Skin lesion analysis toward melanoma detection: A challenge at the 2017 international symposium on biomedical imaging (isbi), hosted by the international skin imaging collaboration (isic),” in *2018 IEEE 15th international symposium on biomedical imaging (ISBI 2018)*. IEEE, 2018, pp. 168–172. 3

19. N. Codella, V. Rotemberg, P. Tschandl, M. E. Celebi, S. Dusza, D. Gutman, B. Helba, A. Kalloo, K. Liopyris, M. Marchetti *et al.*, “Skin lesion analysis toward melanoma detection 2018: A challenge hosted by the international skin imaging collaboration (isic),” *arXiv preprint arXiv:1902.03368*, 2019. 3
20. P. Tschandl, C. Rosendahl, and H. Kittler, “The ham10000 dataset, a large collection of multi-source dermatoscopic images of common pigmented skin lesions,” *Scientific data*, vol. 5, no. 1, pp. 1–9, 2018. 3
21. P. Ngoc Lan, N. S. An, D. V. Hang, D. V. Long, T. Q. Trung, N. T. Thuy, and D. V. Sang, “Neounet: Towards accurate colon polyp segmentation and neoplasm detection,” in *Advances in visual computing: 16th international symposium, ISVC 2021, virtual event, October 4-6, 2021, proceedings, part II*. Springer, 2021, pp. 15–28. 3
22. W. Al-Dhabyani, M. Gomaa, H. Khaled, and A. Fahmy, “Dataset of breast ultrasound images,” *Data in brief*, vol. 28, p. 104863, 2020. 3
23. N. S. An, P. N. Lan, D. V. Hang, D. V. Long, T. Q. Trung, N. T. Thuy, and D. V. Sang, “Blazeneo: Blazing fast polyp segmentation and neoplasm detection,” *IEEE Access*, vol. 10, pp. 43 669–43 684, 2022. 3